



**HAL**  
open science

# **A new instrument for space plasma exploration: The current density coil**

A. Meyer, L. Rezeau, F. Mottez, H. de Feraudy, A. Roux

## ► **To cite this version:**

A. Meyer, L. Rezeau, F. Mottez, H. de Feraudy, A. Roux. A new instrument for space plasma exploration: The current density coil. *Journal of Geophysical Research*, 2001, 106, pp.12999-13006. <10.1029/2000JA900131>. <hal-00405925>

**HAL Id: hal-00405925**

**<https://hal.science/hal-00405925v1>**

Submitted on 11 Jan 2021

**HAL** is a multi-disciplinary open access archive for the deposit and dissemination of scientific research documents, whether they are published or not. The documents may come from teaching and research institutions in France or abroad, or from public or private research centers.

L'archive ouverte pluridisciplinaire **HAL**, est destinée au dépôt et à la diffusion de documents scientifiques de niveau recherche, publiés ou non, émanant des établissements d'enseignement et de recherche français ou étrangers, des laboratoires publics ou privés.



HAL Authorization

# A new instrument for space plasma exploration: The current density coil

A. Meyer, L. Rezeau, F. Mottez, H. de Feraudy, and A. Roux

Centre d'Etude des Environnements Terrestre et Planétaires, Université de Versailles St Quentin en Yvelines, Vélizy, France

**Abstract.** This paper presents an instrument aimed at measuring current densities in space plasmas: a current density coil. Such an instrument already exists for the estimation of currents in the laboratory. A special design has been developed and tested for use on board spacecraft. The characteristics of the instrument are explained in details and many tests performed on the ground are presented. It is shown that the current density coil is sensitive enough to measure ionospheric currents.

## 1. Introduction

A new instrument is proposed to measure current densities in space plasmas: a current density coil (CDC). On existing spacecraft such a measurement has never been included, although attempts to develop a current sensor have already been done. A Danish team is developing a coil based on Faraday rotation of laser light in an optical fiber [Primdahl *et al* 1986]; to our knowledge its sensitivity is around  $10 \mu\text{A m}^{-2}$ . To obtain such a sensitivity a very long fiber has to be used which leads to technical difficulties (the diameter of the coil is around 10 m). Another development of a coil similar to the CDC described here was undertaken by a Russian team [Krasnosel'skikh *et al* 1991], but it has been stopped, and no results are available.

To date, the current density can be derived from particle instruments or magnetometers (DC or AC), but a direct measurement would greatly improve the understanding of the physics. Our aim is to fly this instrument on future spacecraft that will explore regions where the currents are expected to play an important role, mainly in the auroral region, but also in the solar corona. A first set of tests of the coil is presented in this paper, including laboratory tests and numerical simulations.

The paper is organized as follows: After a presentation of the principle on which the instrument works and a short description of its technical realization, the testing equipment and the tests procedures are presented in detail. Then the measurement capabilities of the CDC are described, showing that it is suited for space plasma investigations and that the obtained sensitivity is accurate for the space plasma measurements that should be performed in the future. Of course, since no direct measurement of the current density has ever been performed before, no rigorous comparison can be made; we can only use estimates deduced from other measurements.

Section 5 of the paper is dedicated to an analysis of the limits of the instrument. We study the magnetic field perturbations by the instrument itself, the constraints due to the finite size of the coil, the effects of the potential of the blanket which covers the coil on the electrons that carry the current, and the effect of secondary electrons emitted by the blanket. The study of the effects of variations of the coil potential is important since, in space, it has been shown that the potential of a spacecraft can

vary quite a lot and reach values as high as 100 V [Wahlund *et al*, 1999].

## 2. Description of the Current Density Coils

### 2.1 Physical Principle on Which the Coil Works

The CDC consists of a large number of wire turns wounded on a torus made of magnetic material. As in an electric transformer, an AC current passing through the surface of the torus induces an AC magnetic field in the torus and therefore produces an emf in the winding. The induced emf is,  $e = \mu_0 \mu_r N S R / 2 d \langle j_n \rangle / dt$ , where  $N$  is the number of wire turns,  $S$  is the meridian cross section of the loop,  $R$  is the main radius of the torus, and  $j_n$  is the current density in the direction normal to the loop plane. A consequence of this formula is that the coil is not sensitive to static currents; in fact, as it will be put on board a rocket or a spacecraft, the relative motion of the vehicle with respect to the plasma will provide temporal variations and make the current measurable if its spatial scale is not too large. The principle of the coil is not very different from that of the search coil magnetometers that have been flown on many spacecraft to measure AC magnetic fields [S-300 Experimenters; 1979, Cornilleau-Wehrlin *et al*, 1997]; therefore one might imagine that the CDC is sensitive also to magnetic fields. As will be shown in section 3, a suitable design of the winding gives a strict cancellation of the magnetic flux, thus making the coil sensitive only to AC currents.

As can be seen from the formula given above, a CDC measures the projection of the current density on the direction parallel to its axis. Therefore, to measure the vectorial current density a set of three perpendicular coils is necessary.

### 2.2 Technical Realization

All the figures given in the paper correspond to technical characteristics of the same prototype coil (SN03, diameter 30 cm), although several coils have been tested, with sizes from 8 to 30 cm. The core of the coil is made of a high permeability material (relative permeability  $\mu_r = 250,000$ ) to reach a high sensitivity. The torus shape of the core is obtained by winding a continuous thin sheet of material in a circular shape until a square section of  $\sim 1$  cm side is obtained (Figure 1a.) Two flat washers of the same material are then placed on the top and the bottom of the core to isolate it from external magnetic fields.

Copyright 2001 by the American Geophysical Union.

Paper number 2000JA900131.  
0148-0227/01/2000JA900131\$09.00

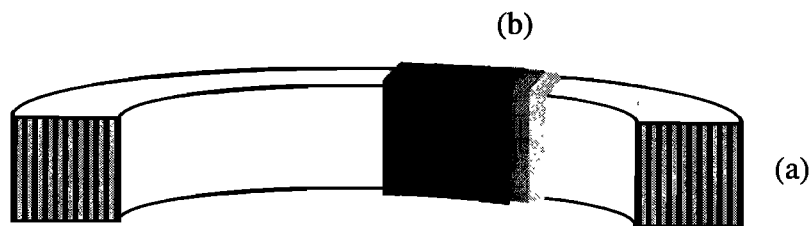


**Figure 1.** Schematic drawing of the coil illustrating (a) the winding of the magnetic material in the core (vertical lines in the cross section), and (b) the successive layers of the wire that make the primary winding.

This torus is then wrapped with two windings (as for search coil magnetometers). The main winding has a very large number of turns (20,000), and it is wound alternately forward and backward to cancel the magnetic flux in the whole winding (Figure 1b). Actually, each layer is equivalent to one turn of radius  $R$  that would be sensitive to DC or AC magnetic fields; by winding an even number of layers, symmetrically, this sensitivity is cancelled [Meyer, 1995]. As shown in Figure 2, the transfer function of this primary winding is a resonance curve with a maximum around 155 Hz, a low-frequency slope of 6 dB/octave (corresponding to the inductive behavior of the coil) and secondary resonances above 4 kHz. To obtain a flat transfer function in a wide frequency range, a secondary winding is used to introduce flux feedback. To smooth the unavoidable secondary resonances, a low-pass filter is added. A high-pass filter is also added, which modifies the low frequency slope to 12 dB/octave; its role is to lower the possible effects of parasitic very low-frequency signals, such as a possible DC drift of the preamplifier or a signal at the spin frequency. Its cutoff frequency is adjusted to the spin frequency of the spacecraft. The resulting transfer function is shown on Figure 2: it is flat over almost three decades. This frequency range can be adjusted to the characteristics of the spacecraft on which the coil is

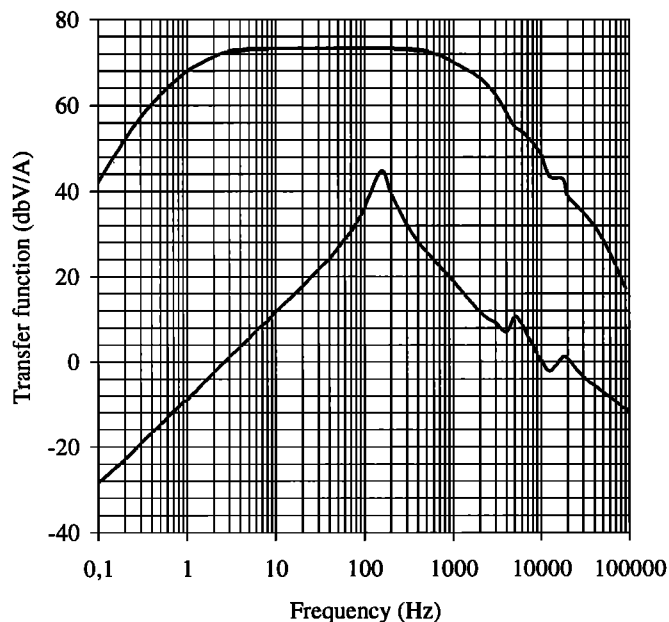


**Figure 2.** Transfer functions of a 30-cm CDC (model SN03). The lowest curve is the response curve of the main winding of the coil alone. The highest one is the final transfer function, when feedback, preamplifier, and filters have been added.

flowed: the low-frequency, cutoff is adjusted to the spin frequency, and the high frequency cutoff depends on the scientific objectives and the regions that will be encountered.

The coil is finally wrapped in a conducting blanket in order to provide a good uniformity of the potential around the probe to minimize the perturbations of the local plasma. In the tests described here the blanket is made of aluminum.

### 3. Means used to test the instrument

The preliminary tests have been performed using an AC current produced in a wire going through the coil. These tests confirm that the principle of the instrument is valid, and they give a calibration of its response, output volts for 1 A current in the wire. They also show that the behavior of the CDC is linear: the response does not depend on the amplitude of the current (provided that the current remains lower than values around 1 A, which is many orders of magnitude higher than the values expected in space). However, as the instrument is dedicated to measurements of currents in space plasmas, these test conditions are oversimplified. To bring complementary information about the workings of the instrument in space conditions, we have used two different means: a test in a plasma chamber and numerical simulations.

#### 3.1. Plasma Chamber

We used the Jonas plasma chamber of Department Environnement Spatial) at Office National d'Etudes et de Recherche Aérospatiales (ONERA) in Toulouse (France). It is a 3-m long stainless steel cylinder in which a cryogenic pumping lowers the pressure to  $10^{-6}$  Pa. The Earth magnetic field is compensated by a set of coils surrounding the chamber. To reproduce realistic space conditions, a plasma can be introduced into the chamber, and an electron gun produces an electron beam. The plasma is an argon plasma, with a density of  $10^5$  cm $^{-3}$  and a temperature of 1500 K. It simulates reasonably well the ionospheric plasma around an altitude of 400 km, except for the magnetic field, which is only a residue of a few microteslas. The electron gun produces a slightly diverging electron beam (its diameter is  $\sim 5$  mm). The energy of the electrons is 3 keV, and they carry a 50  $\mu$ A current. The beam is square modulated at a low frequency which allows one to test the frequency response of the coil on a wide frequency range Reulet *et al.*, [1998].

The current measured by the coil has to be checked against other measurements to be validated. Figure 3 shows a schematic view of the experimental setup. The electron beam goes first through the CDC and then into an 8-cm $^2$  Faraday cage. A fluorescent ZnS disk surrounding the Faraday cage captures the electrons that have missed the cage. Both currents are measured. Also measured is the current flowing in the aluminum blanket

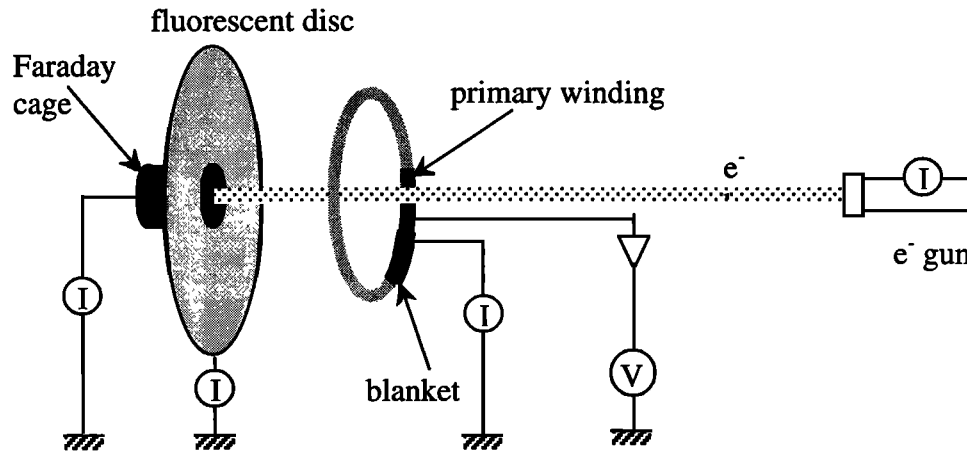


**Figure 3.** Layout of the instruments in the plasma chamber. The CDC is represented by a cut-away sketch, showing the torus of magnetic material, the primary winding, and the conducting blanket.  $I_1$  is the current given by the electron gun,  $I_2$  is the current captured by the Faraday cage,  $I_3$  is the current captured by the fluorescent disk, and  $I_4$  is the current captured by the aluminum blanket of the CDC. The output of the CDC is the voltage of the preamplifier which is connected to the primary winding of the CDC ( $V_C$ ).

covering the CDC, as well as the current given by the electron gun. Thus a complete check of the current balance can be made.

### 3.2. Numerical Simulation

Because the current carried by the electron beam cannot be varied much below  $50 \mu\text{A}$ , the tests performed in the plasma chamber do not give access to the sensitivity of the CDC. That is why numerical simulations have complemented them. These numerical tests also allow separate tests of various effects that influence the behavior of the coil but cannot be distinguished in the plasma chamber experiments.

The simulation box is a 40 cm side cube filled with electrons (we do not consider the behavior of ions, considered as a neutralizing background). These electrons are initialized with random positions, and a Maxwell-Boltzmann velocity distribution, characterized by a uniform average density, a parallel bulk velocity, and an isotropic temperature. Because of the electron bulk velocity, this distribution carries a current. The electrons are moving in external (not self-consistent) constant magnetic and electric fields. These fields consist of a uniform ambient magnetic field (parallel to the initial current), plus a perturbation generated by the high permeability material (the core of the loop), and an electric field caused by a potential drop between the coil and its environment (this field is the solution of the Laplace equation in vacuum; it does not take into account the ambient plasma).

The CDC is placed in the middle of this box: It is a toroidal loop with a square cross section, similar to the real one. The comparison is made between the ambient ideal current density determined by the initial conditions of the plasma and the current density flowing through the coil, obtained by counting the electrons that cross the section defined by the inner part of the loop. The discrepancy gives an indication of the error made when using the CDC. In the simulation, unlike in real tests, several effects can be switched off to understand their specific role: (1) the perturbing magnetic field due to the magnetic core of the coil and (2) the capture of the electrons which hit the coil. If effect 2 is switched off, the coil becomes transparent to electron motion. Finally, the electric potential of the coil can be set to three different values: 0, +10 V, and -100 V.

### 3.3 Comparison of the Different Methods of Measuring the Current

In real life, in space, the current structure, whatever it is (tube, sheet, etc...), extends over distances much larger than the size of the coil. Although no direct current measurements have ever been performed, this assumption seems quite reasonable. Previous estimates made by particle or magnetic field experiments indicate that scales as low as 100 m at an altitude of 400 km can be expected [Forget *et al.*, 1991]. Some authors suggest that 100 m could be the smallest scale [Staciewicz and Potemra, 1998] which can be related to the fact that the inertial length of the electrons at this altitude is around 100 m and that it is the smallest physically significant scale. Observations of the thickness of auroral arcs made from the ground give the same order of magnitude [Borovsky, 1993]. Therefore, in any case, the CDC will pass through current structures much larger than its own diameter and will "catch" a small section of the current and give a measure of the current density times its section.

In the numerical simulation the situation is similar except for one difference: There is only an electron beam present in the simulation box, and its charge is compensated by a stationary ion background, and no space charge field is taken into account.

In the plasma chamber experiment, however the relative dimensions of the coil and the current are reversed: the electron beam covers only  $\sim 0.1\%$  of the section of the coil. To explore the whole surface and especially to study the edge effects, the coil is translated in front of the electron beam.

## 4. Measurement Capabilities

### 4.1. Preliminary Tests in the Plasma Chamber Without Plasma

With an electron beam carrying  $50 \mu\text{A}$ , a numerical simulation shows that the current density is measured with a precision of 0.5%. With the real coil, we have to compare the obtained response in the chamber to a reference response. Calibrated with a current produced in a wire, the obtained reference transfer function at 55 Hz (in the flat part of the function) is  $4640 \text{ V A}^{-1}$ , that is  $73.3 \text{ dBV A}^{-1}$ , when the potential

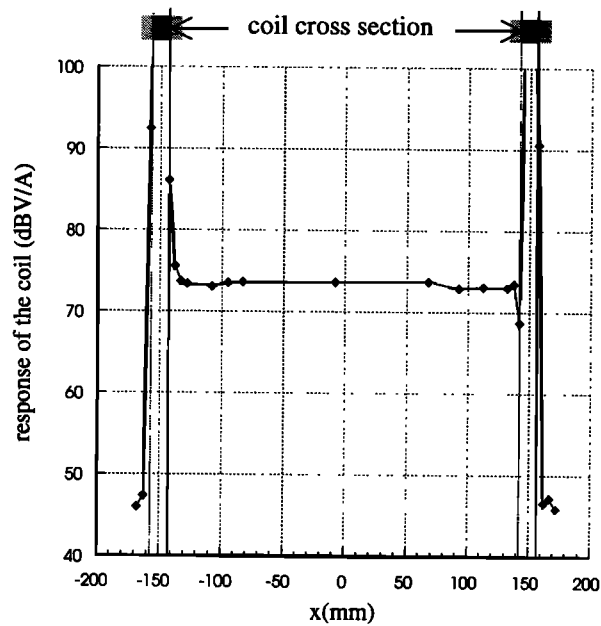


**Figure 4.** Response of the CDC as a function of the position of the incident electron beam (model SN03). The size of the coil is superimposed (dark shaded squares). The light shaded regions have the size of the beam.

of the coil is fixed at 0 V. In the plasma chamber the current is measured with the Faraday cage ( $I_2$ ); we obtain  $I_2 \approx 30 \mu\text{A}$  for the 55-Hz part of the signal. This is consistent with the results expected for the first harmonic frequency of a 55-Hz square signal of amplitude switching from 0 to 50  $\mu\text{A}$ . The current through the fluorescent disk is stable around 0.2  $\mu\text{A}$  and therefore always negligible compared to the measured current. The current through the aluminum blanket of the coil is equal to 0 except when the beam hits the coil. The coil is moved perpendicular to the electron beam, and its response is plotted in Figure 4, where the size of the coil is shown for comparison. When the beam passes in the central region of the coil (between +130 and -130 mm), the transfer function varies between 72.88 and 73.69 dBV/A, with an average of 73.4 dBV  $\text{A}^{-1}$ , which represents an accuracy of less than 1%. When the beam hits the

coil, the measurement is disturbed because the current through the aluminum shield reaches 15  $\mu\text{A}$ . The asymmetry in the response near the two edges of the coil is likely to be due to a slight curvature of the beam (due to the magnetic field residue). This is not comparable to the situation in space, where electrons will continuously hit the whole surface of the coil; the shield is designed with one strip over each of the four sides of the torus to ensure a symmetry of the currents with respect to the axis of the coil and therefore a balance of the currents in the shield.

#### 4.2. Tests in the Presence of a Plasma

First of all, the CDC will be used in plasmas and therefore has to be tested in the plasma chamber filled with plasma. In that case, with the same current density as before and the potential of the coil fixed to 0 V, the transfer function in the center of the coil is 73.3 dBV  $\text{A}^{-1}$ , which is the nominal result. It is interesting to note that the edge effects are less important when the coil is embedded in a plasma: Considering the case where the beam is only 5 mm from the coil (if it is closer the current flows through the shield), the departure from the central measurement is 8.6% without plasma and only 3.2% with plasma. This improvement is likely to be due to the screening of the coil by the plasma, but it cannot be tested properly since the Debye length ( $\approx 8$  mm) is of the same order as the beam.

#### 4.3. Comparison of the Measurement Capabilities With the Known Values of Currents in Space Plasma

It must be noted that the current carried by the electron beam in the plasma chamber (50  $\mu\text{A}$ ) corresponds to high values of the current density: around 700  $\mu\text{A m}^{-2}$  if one assumes that the coil is embedded in the current. In the auroral region the estimates of the current are deduced from the magnetic measurements, and the maximum values of the currents are expected to be around 300  $\mu\text{A m}^{-2}$  at the subkilometer scale [Berthelier *et al.*, 1991; Staciewicz and Potemra, 1998]. Therefore the CDC must be able to measure current densities significantly lower than those tested in the plasma chamber. In the numerical simulation it is not difficult to decrease the current and to show that the coil can measure much smaller currents: a 1  $\mu\text{A m}^{-2}$  current is measured with an accuracy of 0.2%.

The sensitivity of the real coil can be tested in the laboratory, in a magnetic environment that is cleaner than in a large plasma

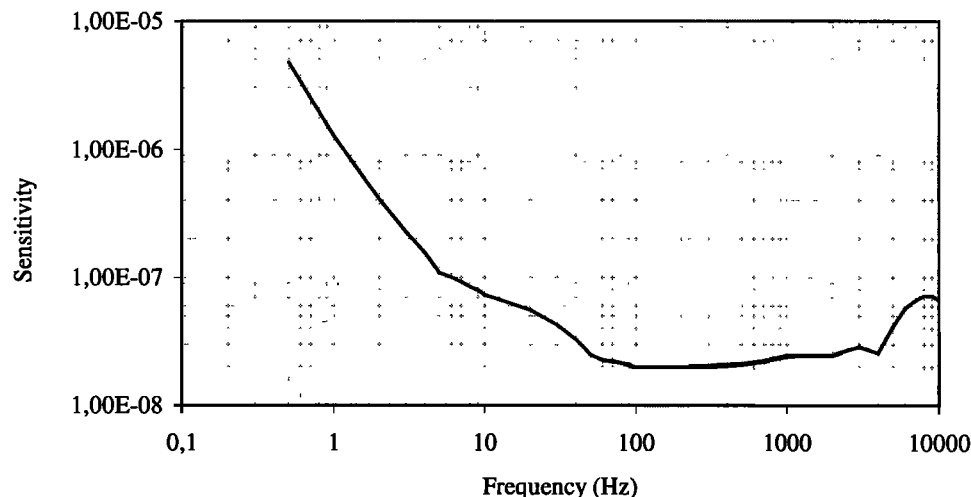


**Figure 5.** Sensitivity (in  $\text{A m}^{-2} \text{Hz}^{-1/2}$ ) of a 30-cm coil, with a 20,000 turns winding (model SN03).

chamber. The result obtained under these conditions is plotted in Figure 5 and it can be compared to the estimates of currents in space. If a relative velocity of the spacecraft and a current structure of  $1 \text{ km s}^{-1}$  is assumed, a 100-m structure is crossed in 0.1 s and appears as a 10-Hz signal. For a current density of  $200 \mu\text{A m}^{-2}$  [Forget *et al.*, 1991] and an analysis with a 50% bandwidth, the coil needs a  $100 \mu\text{A m}^{-2} \text{ Hz}^{1/2}$  sensitivity to be able to detect the current structure. As shown in Figure 5, the CDC allows measurements of much smaller current density values in that frequency range. Of course, the figures given here depend on the velocity of the spacecraft and on the characteristics of the analysis and, hence the real sensitivity of the coil might be slightly different. Nevertheless, it clearly evidences that the instrument has the capability of studying ionospheric currents. This curve also shows that structures smaller than 100 m will also be resolved by the instrument (corresponding to higher frequencies), thus allowing the exploration of a scale domain which so far has not been explored.

## 5. Exploration of the limits of the instrument

### 5.1. Magnetic Perturbations Due to the Coil Material

The magnetic material, which is the core of the CDC, creates its own magnetic moment, which modifies the field lines of the nearby external magnetic field. Of course, with a real coil this effect cannot be avoided. In the numerical simulations it can be removed, since the measurements are made by counting the particles going through the coil and not by measuring the induced voltage. One can expect that the modification of the field lines will be more important if the external field lines are far from normal to the coil plane. This effect is tested in Figure 6, where a current of  $1 \mu\text{A m}^{-2}$  is flowing through the coil at different angles. When the angle between the current and the magnetic field is small, there is no difference between the two

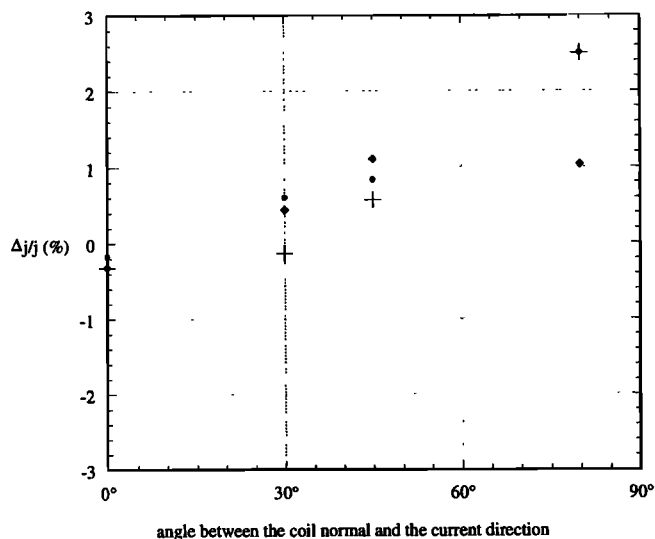


**Figure 6.** Error on the measurement of the current deduced from numerical simulations. Diamonds correspond to the case where the coil is transparent and there is no perturbing magnetic field, pluses correspond to the case where the coil is transparent and the magnetic field of the magnetic core is present, and dots correspond to the most realistic case where the coil is thick and the field is perturbed.

cases, with or without the perturbing magnetic field. When the angle is large ( $80^\circ$ ), the part of the current that is measured is small, and the error on the measurement reaches 2.5%. As will be shown in section 5.2, when the coil is in a set of three coils, this error plays a minor role since it modifies a very small component only. In the other case, when only one coil is used, this error is more important since it cannot be corrected as the direction of the current is unknown.

### 5.2. Geometrical Effects

The finite size of the CDC introduces some unavoidable limitations. First, as already mentioned, a given coil measures only the component of the current density that is normal to its surface, but as the angle with the normal increases, the error on the measurement also increases. The finite size of the section of the torus induces a loss of the particles that hit the inner side of the sensor, giving rise to a dead angle (assuming that the particles are captured and that no secondary emission occurs). For a 30-cm coil this angle is equal to  $87^\circ$ . For angles smaller than this limit but still far from the normal of the loop, the thickness of the coil induces an error on the estimate of the surface "seen" by the current. This surface is smaller than the expected value of  $\pi R^2 \cos \alpha$  and has to be used to deduce the current density from the current measured by the loop. As shown in Figure 6, this error is smaller than the error due to the perturbing magnetic field, and the combination of both effects gives an accuracy of 2.5% for the measurement at  $80^\circ$ . These effects are drawbacks if the instrument is made up of only one coil. If, however, it is a set of three orthogonal coils, the error can be corrected. A first estimate of the direction of the current can be calculated; then, knowing its direction relative to one coil, the error on the corresponding surface can be corrected, and a refined estimate of the direction can be deduced. As soon as the current density direction is close to the normal of one of the three coils, the precision of the estimate will be excellent since the maximum error will be on very small components. The worst situation would be when the current is as far as possible from all the normals, that is around  $55^\circ$ , but then the error is less than 1% and can be corrected.

These orders of magnitude are given for a 30-cm-diameter coil. Clearly, they increase if the coil is smaller, because it is not possible to reduce the section of the coil in proportion to the radius of the torus, for obvious technical reasons. However, even in that case, the geometrical errors can be corrected.

Changing the size of the coil has a consequence on its sensitivity. The sensitivity shown here (Figure 5) is that of a 30-cm coil with 20,000 wire turns. It can be compared to the sensitivity of a 15 cm coil with 16,300 wire turns (Figure 7); there is a loss of  $\sim 1$  decade in sensitivity when the dimension is reduced by a factor of 2. When the use of the coil fixes its size (for instance a large coil cannot be flown on a rocket), the sensitivity can be improved by increasing the number of wire turns. A new 15-cm coil is being built, with 40,000 wire turns; its sensitivity is expected to reach a value equal to twice the sensitivity of the 30 cm coil. Therefore, although it will be less sensitive than a 30-cm coil, it will be much better than the previous 15-cm coil.

### 5.3. Influence of the Electrostatic Potential of the Coil

All the tests that have been discussed in the previous sections were performed with a grounded conducting blanket. With the coil on board a spacecraft the problem will be more complicated

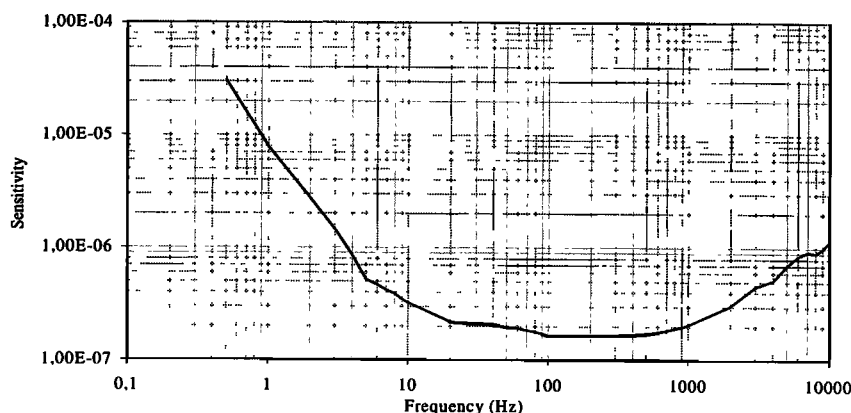


Figure 7. Sensitivity (in  $\text{A m}^{-2} \text{Hz}^{-1/2}$ ) of a 15-cm coil with 16,300 wire turns.

since there is no ground and the ambient plasma influences the potential of the instruments. Therefore tests have been performed in the plasma chamber together with numerical simulations with different potentials of the coil, including the floating potential.

In the chamber, introducing a power supply in the branch where  $I_4$  is measured (see Figure 3) can modify the voltage of the coil aluminum blanket. The plasma potential is measured during the experiments by a Langmuir probe; its value is around 0.6 V. When the potential of the blanket is left floating, it reaches a value, around -0.6 V, which is a bit less than the plasma potential; i.e., the coil behaves like a Langmuir probe. Figure 8 shows the response of the CDC for different values of the voltage of the coil blanket, with and without plasma in the chamber. The main conclusion deduced from these tests is that the reference response is obtained only when the potential of the coil is kept near 0 V. When it moves away from this value, the response varies considerably. Therefore, to obtain precise measurements in space, the voltage of the coil should be kept at the spacecraft potential. Another interesting conclusion of this study is about the edge effects. When the coil is tested in a

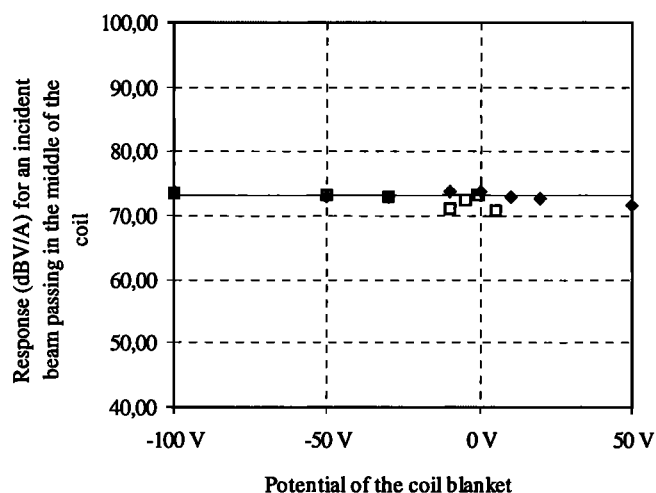


Figure 8. Response of the CDC in the plasma chamber as a function of the voltage of the conducting blanket of the coil, with plasma in the chamber (open squares) or without (solid diamonds). The thin line represents the nominal response (model SN03).

plasma, there are less edge effects: The beam can pass closer to the coil without being affected by it. This result, already evidenced at 0 V, is also valid at other voltages.

All these tests in the plasma chamber have been performed with the same 3-keV electron beam. Of course, the influence of the voltage of the coil on the beam is strongly related to the energy of the particles and to their charge. For a current carried by ions the above results should be reversed. The relative effects of the voltage of the coil and the energy of the electrons have been tested in numerical simulations. The results are presented in Figure 9, which shows that the error on the estimate of the current density increases when the energy of the beam decreases. They also show that for low voltages the error becomes large only for very low energies. On the other hand, for a -100-V voltage the error is higher than 5% as soon as the energy of the beam is less than a few 100 eV. These observations are consistent with an electrostatic interaction between the beam and the coil. This means that with the real coil in the plasma chamber the physical situation is more complicated, since the variations are not consistent with the simple electrostatic interaction. This difference is very likely due to the existence of secondary electrons emitted by the coil itself, since in the numerical simulation this effect is not included. Taking this effect into account, the results in Figure 8 become more clear: For a positive voltage the secondary electrons are recaptured after a short flight, and for a negative potential the electrons are repelled from the coil and perturb the estimate of the current. For a very negative voltage they are strongly repelled from the coil and hence do not disturb any longer the response of the coil; it goes very close to the nominal one.

#### 5.4. Perturbation of the Measurement by Secondary Electrons and Photoelectrons.

As evidenced by the results shown in section 5.3, the emission of secondary electrons is an important problem to consider in order to understand the behavior of the coil in all situations. A similar problem in space, which has not been tested on the ground, is the emission of photoelectrons. The secondary-electron emission yield has been studied for many elements and compounds: All show the same kind of response, an increasing emission as a function of the energy of the incident electrons to a maximum yield and then a decrease [Scholtz *et al.*, 1996]. This maximum yield and the corresponding incident energy then characterize a given element. For aluminum the maximum yield

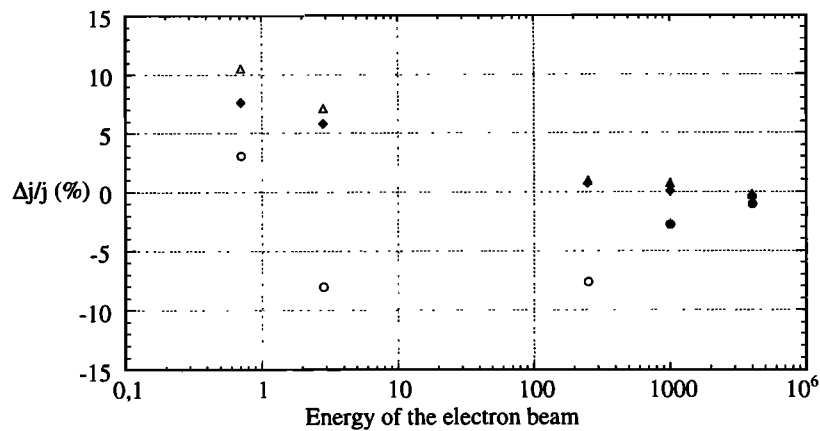


**Figure 9.** Error on the measurement of the current deduced from numerical simulations as a function of the energy of the electron beam. The diamonds correspond to a grounded coil, the triangles correspond to a +10-V voltage, and the dots correspond to a -100 V voltage. The symbols are solid when the energy of the beam is higher than the voltage of the coil, and they are open when it is of the same order of magnitude or lower.

is around 1 and is obtained for 300-eV electrons; for 3-keV electrons the yield goes down to 0.6 [Garrett, 1980].

An estimate of the number of secondary electrons that are emitted by the coil blanket can be made, taking into account the geometry of the instrument and the known dependency of the yield as a function of the incidence angle [Vaughan, 1989]. The coil is covered by four strips of aluminum, one on each side of the torus. It is most likely that the electrons produced by the outside, top side, and bottom side will not disturb the current measurement to any large extent. The main perturbation will come from the inner side. As this surface is a cylinder, the incidence angle depends on the point of incidence. By performing integration on the entire surface, we obtain a 7% effective yield for the coil. This value corresponds to a normal incidence of the current with respect to the coil, as it was in the plasma chamber experiment. If we study the secondary emission as a function of the angle between the current and the normal to the coil, we find that it is stable for angles smaller than 45°, while for larger angles it increases to 50% for an angle of 80°. Therefore this emission becomes a large source of error in the measurements for very large incidence angles. The error behaves in a similar way to the geometrical effect studied above; that is, if there is a set of three coils on board the spacecraft, it is a minor problem.

One can think of reducing the effect of the secondary electrons by choosing the best material for the cover. A comparative study of many elements [Whetten, 1962] shows that carbon has the smallest efficiency, 0.45, obtained for a 500-eV energy when it is in soot form. A similar study for photoemission of amorphous materials [Grard, 1973] shows that graphite is the material that produces the smallest number of photoelectrons. Therefore we have decided to change the conducting blanket of our coils and replace aluminum with carbon. Preliminary tests show that the voltage of the blanket (if it is left floating) reaches the plasma potential with a much better accuracy, which should minimize the effects of secondary electrons.

## 6. Conclusion

The tests which have been presented here show that the CDC is a new instrument that is capable of improving our knowledge

of space plasma properties. First of all, it is sensitive enough to measure the current densities that are expected in the auroral region, as far as we know. It will also make possible the exploration of smaller scales than the scales that can be studied using magnetometers, that is, scales that have never been explored before. The sensitivity of the coil is higher when the coil is larger; therefore the size chosen for a given spacecraft has to be a compromise between sensitivity and bulk, although small coils can be improved by increasing the number of winding turns.

Clearly, the number of CDCs on board the spacecraft is also very important. A set of three coils will always give a good estimate of the direction and the intensity of the current density. On the other hand, a single coil will give only an estimate of the projection of the current density with an error which might be very large if the angle of the current direction and the coil normal is large.

The tests performed on the coil show that its response is more reliable when its potential is maintained close to 0 V, which in the case of the plasma chamber was close to the plasma potential. This indicates that in a space experiment the potential of the coil should be kept at the spacecraft potential. When the voltage of the coil departs from the ground potential, the effects of secondary electrons or photoelectrons become more important. This problem is still under study, and some improvements can be included in future models, such as a carbon blanket instead of an aluminum one for instance.

A set of three CDC is going to be flown in December 2001 on a rocket launched in the cusp region. A full set of plasma instruments will be on board: particle measurements and DC and AC magnetic field measurements. This will allow a detailed comparison of the current estimates obtained by these three different means. Particle instruments can give a direct estimate of the current density, but they suffer from limitation in time resolution (due to the time needed to sample all directions and energies) and from the thresholds in energy. On the other hand, magnetometers have a high time resolution but give only an indirect estimate of currents since the relation between currents and field is differential. Owing to these limitations, the results from these two instruments will allow one to check some properties of the currents, but will not be redundant with the CDC measurements.

**Acknowledgments.**

The tests in the plasma chamber have been performed with financial support of the French space agency, CNES, and of Université de Versailles-Saint-Quentin en Yvelines. The authors wish to thank François Lefeuvre and Vladimir Krasnosel'skikh for fruitful discussions, and Bernard Poirier, Dominique Alison, and the ONERA team for their technical support. The computations have been supported by the CNRS and made on a Cray 98 at IDRIS (Orsay, France)

Michel Blanc thanks the referees for their assistance in evaluating this paper.

**References**

- Berthelier, A., J.C. Cerisier, J.J. Berthelier, and L. Rezeau, Low frequency magnetic turbulence in the high-latitude topside ionosphere: low-frequency waves or field-aligned currents, *J. Atmos. Terr. Phys.*, *53*(3/4), 333-341, 1991.
- Borovsky, J. E., Auroral arc thickness as predicted by various theories, *J. Geophys. Res.*, *98*, 6101-6138, 1993.
- Comilleau-Wehrin, N., et al., The CLUSTER spatio-temporal analysis of field fluctuations (STAFF) experiment, *Space Sci. Rev.*, *79*(1-2), 107-136, 1997.
- Forget, B., J.-C. Cerisier, A. Berthelier, and J.-J. Berthelier, Ionospheric closure of small-scale Birkeland currents, *J. Geophys. Res.*, *96*, 1843-1847, 1991.
- Garrett, H. B., Spacecraft charging: a review, *Space Systems and their interactions with earth's space environment, Progress in astronautics and aeronautics*, vol. 71, edited by H. B. Garrett and C. P. Pike, published by American Institute of Aeronautics and Astronautics, New York, 1980.
- Grard, R. J. L., Properties of the satellite photoelectrons sheath derived from photoemission laboratory measurements, *J. Geophys. Research*, *78*, 2885-2906, 1973.
- Krasnosel'skikh, V.V., A.M. Natanzon, A.E. Reznikov, A. Y. Schyokotov, S.I. Klimov, A.E. Kruglyi, and L. Woolliscroft, Current measurements in space plasmas and the problem of separating between spatial and temporal variations in the field of a plane electromagnetic wave, *Adv. Space Res.*, *11*, (9), 37-40, 1991.
- Meyer, A., Boucle de courant à contre réaction de champ, note technique, Centre d'Etude des Environ. Terr. et Planét., Vélizy, France, 1995.
- Primdahl, F., P. Hoeg, C. J. Nielsen, and J. E. Schroder, A new method for measuring space plasma current densities by the Faraday rotation of laser light in optical monomode fibers, *DRI Sci. Rep.* 4-86, 1986.
- Reulet, R., L. Levy, and D. Sarrail, Etude du comportement d'une boucle de courant en présence d'un plasma ionosphérique, Assistance technique simulation spatiale, *Rapp. ONERA RF/470900/470901*, 1998.
- S-300 Experimenters, Measurements of electric and magnetic wave fields and of cold plasma parameters on-board GEOS 1. Preliminary results, *Planet. Space Sci.*, *27*, 317-339, 1979.
- Scholtz, J. J., D. Dijkkamp, and R. W. A. Schmitz, Secondary electron emission properties, *Philips J. Res.*, *50*, 375-389, 1996.
- Staciewicz, K., and T. Potemra, Multiscale current structures observed by Freja, *J. Geophys. Res.*, *103*, 4315-4325, 1998.
- Vaughan, J. R. M., A new formula for secondary emission yield, *IEEE Trans. Electron Devices*, *36*, 1963-1967, 1989.
- Wahlund, J. E., L. J. Wedin, T. Carrozi, A. I. Eriksson, L. Anderson, and H. Laasko, Analysis of Freja charging events, *IRF Sci. Rep.* 253, 1999.
- Whetten, N. R., Secondary electron emission, *Methods of Experimental Physics*, vol. 4, Academic, San Diego, Calif., 1962.

---

H. de Feraudy, A. Meyer, F. Mottez, L. Rezeau, and A. Roux, CETP/UVSQ, 10-12 avenue de l'Europe, Vélizy, France. (rezeau@cetp.ipsl.fr)

(Received May 31, 2000 ; revised September 5, 2000, accepted September 5, 2000.)